

QSAR studies of some anilinoquinolines for their antitumor activity as EGFR inhibitors

Shweta Sharma^{1*}, Vijay K. Agrawal², Basheerulla Shaik², and Anita K.³

^{1,3}Department of Chemistry, Career College, Bhopal-462002, Madhya Pradesh, India

²National Institute of Technical Teachers' Training & Research, Bhopal

Abstract: Quantitative Structure-Activity Relationship studies has been performed on some anilinoquinolines. A variety of parameters including 2D- autocorrelation, RDF, 3D- MoRSE, WHIM and GETAWAY parameters have been chosen for modeling the antitumor activity of these compounds. The multiple regression analysis reveals that the seven –parametric model is the best for modeling the activity of the compounds under present study. This model has been tested by using cross validated parameters. The results are also discussed on the basis of ridge regression.

Keywords: QSAR, NCSS, EGFR, Ridge regression.

I. Introduction

Cancer is now a day's used as a generic term describing a group of about 120 different diseases, which can affect any part of the body and defined as the state characterized by the uncontrolled growth and invasion of normal tissues and spread of cells [1]. According to WHO reports cancer is a leading cause of premature death worldwide, accounting for 7.6 million deaths (around 13% of all deaths) only in 2008. The deaths from cancer worldwide are projected to continue rising, reaching an estimated 13.1 million in 2030 (WHO 2012) [2]. A number of natural and synthetic products have been found to exhibit anticancer activity against tumor cell lines [3-7].

It is worth mentioning that epidermal growth factor receptor (EGFR) is a rational target for antitumor strategies. The EGFR is expressed or highly expressed in a variety of human tumors including non-small cell lung cancer (NSCLC), breast, head and neck, gastric, colorectal, esophageal, prostate, bladder, renal, pancreatic, and ovarian cancers [8]. Particularly, a large number of compounds have been synthesized and evaluated as EGFR inhibitors, with special attention being paid to compounds having a phenyl amino pyrimidine moiety in their structures [9-13]. Evidently Anilinoquinolines are well known EGFR inhibitors as demonstrated in various studies [14-16]. In silico QSAR studies were performed by Pasha et al., [17] on a series of EGFR inhibitory anilinoquinolines. In the study they have reported HQSAR, DFT-based QSAR, ligand – based 3D- QSAR, and receptor- guided HQSAR analysis of 58 anilinoquinoline derivatives using various parameters. In the present study we are also using the same data set of compounds with pIC₅₀ activities, but selecting different independent variables.

II. Computational Details

The structural details of the 58 anilinoquinolines derivatives with EGFR inhibitory activity pIC₅₀ have been reported in table 1. The calculated parameters have been summarized in table 2. From the large pool of 2D-autocorrelation parameters, RDF, 3D MoRSE, WHIM and GETAWAY descriptors we have selected a few to carryout multiple regression analysis using variable selection method. For calculating the parameters we have used Dragon software [18]. From all the calculated descriptors, useful descriptors were generated by variable selection of descriptors in multiple regression analysis using NCSS software [19]. The intercorrelatedness among the descriptors and their correlation with the activity values pIC₅₀ is presented in Table 3. All the statistically significant models along with their quality have been summarized in table 4. This table also includes the values of Pogliani's quality factor Q [20-22], which is the ratio of R and Se ($Q = R/Se$).

III. Results and Discussion

The regression analysis of the data set yielded several statistically significant models. However, on the basis of highest R² value, we propose following statistically significant models to be best for modeling the EGFR inhibitory activity:

Five variable model (Model no.5, Table no.4)

The Five -parametric model having maximum R² value 0.7779 is as below:

$$\text{pIC}_{50} = -22.2852(\pm 3.3394) \text{G3m} - 7.6033(\pm 0.8275) \text{MATS1e} + 8.2819(\pm 1.6698) \text{MATS3p} + 0.0356(\pm 0.0101) \text{RDF095s} - 0.4418(\pm 0.1033) \text{RDF110u} + 12.9503 \quad (1)$$

N=58, R² =0.7779, R²_A = 0.7566, Se= 0.0930, F= 36.429, Q = 9.484

Six variable model (Model no.6 , Table no.4)

When H1i is added to the above model a six-parametric model with $R^2 = 0.8177$ is obtained as below:

$$pIC_{50} = -18.9191(\pm 3.2170) G3m + 1.6503(\pm 0.7941) H1i - 7.4943(\pm 0.7577) MATS1e + 9.8815(\pm 1.6009)$$

$$MATS3p + 0.0477(\pm 0.0099) RDF095s - 0.4949(\pm 0.0958) RDF110u + 5.4334 \quad (2)$$

$$N=58, R^2 = 0.8177, R^2_A = 0.7963, Se = 0.0851, F = 38.134, Q = 10.626$$

Seven variable model (Model no.7 , Table no.4)

When Mor29u combined with the above six-parametric model a seven-parametric model is yielded with improved R^2 value.

$$pIC_{50} = -20.5758(\pm 2.8191) G3m + 3.2238(\pm 0.7024) H1i - 7.4577(\pm 0.6576) MATS1e + 11.0537(\pm 1.4168)$$

$$MATS3p - 2.1918(\pm 0.5205) Mor29u + 0.0607(\pm 0.0091) RDF095s - 0.7058(\pm 0.0971) RDF110u + 4.8803$$

(3)

$$N=58, R^2 = 0.8654, R^2_A = 0.8466, Se = 0.0738, F = 45.943, Q = 12.605$$

It is evident that the value of R^2 is drastically increases from six-parametric model to the seven-parametric model. This means that seven-variable model is statistically better than previous one. Consequently, we observed that the seven-parametric model is the best for modeling the activity.

Further confirmation is obtained by estimating the pIC_{50} activity using model- 7 which is reported in Table 5. The estimated values are in good agreement with observed values. When observed activity values are plotted against estimated values, we obtained a graph which is reported in Fig. 2. The predictive power of the model comes out to be 0.8654. To validate the obtained model cross validation has been done by LOO method, and obtained values are reported in table 6. The highest R^2_{CV} for the model 7 shows that this is the most appropriate model for modeling pIC_{50} value of compounds used in the present study. For any kind of possible defect we have calculated variance inflation factor, tolerance and condition number for various parameters using VIF plot which is given in Table 7. All the parameters show the value within the permissible limit. Therefore, the model is free from any kind of defect. Ridge trace suggests that there is no co-linearity in the model.

IV. Conclusion

1. 2D –autocorrelation, RDF, 3D MorSE and GETAWAY parameters are the useful parameters for modeling the EGFR inhibitory activity for the present set of compounds.
2. MATS1e and MATS3p plays a dominating role for prediction of antitumor activity.

Acknowledgement

The corresponding author is thankful to UGC. This work was financially supported by the UGC MRP.

References

- [1]. C.H. Yarbro, M. Goodman, M.H. Frogge. *Cancer Nursing Principles and Practice* (6th edition); Boston, Jones & Bartlett Publishers. (2005), 1879, ISBN 0815169906.
- [2]. J. Ferlay, H.R. Shin, F. Bray, D. Forman, C. Mathers, D.M. Parkin, GLOBOCAN 2008 v1.2. Cancer Incidence and Mortality Worldwide: IARC CancerBase No. 10. Lyon, France: International Agency for Research on Cancer, Available from: <http://globocan.iarc.fr>, accessed on day/month/year. (2010).
- [3]. M.E. Bracke, R.M.L. Van Cauwenberge, M.M. Mareel, *Clin. Metastasis*, 2, (1984), 161.
- [4]. R. Giavazzi, A. Garofalo, G. Damia, S. Garattini, M. D'Incalci, *British J. of Cancer*, 57(3), (1988), 277.
- [5]. S. Mukherjee, V. Kumar, A.K. Prasad, H.G. Raj, M.E. Bracke, C.E. Olsen, S.C. Jain, V.S. Parmar, *Bioorg. Med. Chem.*, 9(2), (2001), 337.
- [6]. B.W. Vanhoecke, H.T. Depypere, A. De Beyter, S.K. Sharma, V.S. Parmar, D. De Keukeleire, M.E. Bracke, *Pure App. Chem.*, 71(1), (2005), 65.
- [7]. L. Sartor, E. Pezzato, I. Dell'Aica, R. Caniato, S. Biggin, S. Garbisa, *Biochem. Pharm.* 64(2), (2002), 229.
- [8]. D.S. Salomon, R. Brandt, F. Ciardiello, *Crit. Rev. Oncol. Hematol.* 19, (1995), 183-232.
- [9]. G.W. Rewcastle, W.A. Denny, A.J. Bridges, H.R. Zhou, D.R. Cody, A. McMichael, D.W. Fry, *J. Med. Chem.*, 38, (1995), 3482–3487
- [10]. A.M. Thompson, A.J. Bridges, D.W. Fry, A.J. Kraker, W.A. Denny, *J. Med. Chem.*, 38, (1995), 3780–3788.
- [11]. J.B. Smaill, B.D. Palmer, G.W. Rewcastle, W.A. Denny, D.J. McNamara, E.M. Dobrusin, A.J. Bridges, H.R. Zhou, H.D.H. Showalter, R.T. Winters, W.R. Leopold, D.W. Fry, J.M. Nelson, V. Slintak, W.L. Elliot, B.J. Roberts, P.W. Vincent, S.J. Patmore, *J. Med. Chem.* 42, (1999), 1803–1815.
- [12]. G.W. Rewcastle, B.D. Palmer, A.J. Bridges, H.D.H. Showalter, S. Li, J. Nelson, A. McMichael, A.J., Kraker, D.W. Fry, W.A. Denny, *J. Med. Chem.*, 39, (1996), 918–928.
- [13]. J.B. Smaill, H.D.H. Showalter, H.R. Zhou, A.J. Bridges, D.J. McNamara, D.W. Fry, J.M. Nelson, V. Sherwood, P.W. Vincent, B.J. Roberts, W.L. Elliott, W.A. Denny, *J. Med. Chem.* 44, (2001) 429–440.
- [14]. H. Assefa, S. Kamath, J.K. Buolamwini, *J. Comp. Aided Mol. Des.*, 17, (2003), 475–493.
- [15]. D.V. Pednekar, M.A. Kelkar, S.R. Pimple, K.G. Akamanchi, *Med. Chem. Res.*, 13, (2004), 605–618.
- [16]. J. Stamos, M.X. Sliwkowski, C. Eigenbrot, *J. Biol. Chem.*, 277, (2002), 46265–46272.
- [17]. F.A. Pasha, M. Muddassar, A.K. Srivastava, S.J. Cho, *J. Mol. Model.* 16, (2010), 253-277.
- [18]. DRAGON software for calculation of topological indices, www.disat.unimib.it
- [19]. NCSS statistical analysis software, www.ncss.com
- [20]. L. Pogliani, *AminoAcids*, 6, (1994), 141.
- [21]. L. Pogliani, *J. Phys. Chem.*, 100, (1996), 18065.
- [22]. L. Pogliani, *Chem. Rev.*, 100, (2000), 3827.

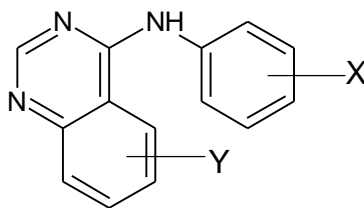


Fig.1 Basic structure of anilinoquinolines.

Table .1 Structural details and pIC_{50} values for the compounds used in present study.

Compound no.	X	Y	pIC_{50}
1	H	H	6.46
2	3-F	H	7.25
3	3-Cl	H	7.64
4	3-Br	H	7.57
5	3-I	H	7.1
6	3-CF ₃	H	6.24
7	H	6-OMe	7.26
8	3-Br	6-OMe	7.52
9	H	6-NH ₂	6.11
10	3-CF ₃	6-NH ₂	6.24
11	3-Br	6-NH ₂	9.11
12	H	6-NO ₂	5.3
13	3-Br	6-NO ₂	6.05
14	H	7-OMe	6.92
15	3-Br	7-OMe	8
16	H	7-NH ₂	7
17	3-F	7-NH ₂	8.7
18	3-Cl	7-NH ₂	9.6
19	3-Br	7-NH ₂	10
20	3-I	7-NH ₂	9.46
21	3-CF ₃	7-NH ₂	8.48
22	H	7-NO ₂	4.92
23	3-F	7-NO ₂	5.22
24	3-Cl	7-NO ₂	6.09
25	3-Br	7-NO ₂	6
26	3-I	7-NO ₂	6.27
27	H	6,7-di-OMe	7.54
28	3-F	6,7-di-OMe	8.42
29	3-Cl	6,7-di-OMe	9.51
30	3-Br	6,7-di-OMe	10.6
31	3-I	6,7-di-OMe	9.05
32	3-CF ₃	6,7-di-OMe	9.62
33	3-Br	6-NHMe	8.4
34	3-Br	6-NMe ₂	7.08
35	3-Br	7-OH	8.33
36	3-Br	7-NHMe	8.16
37	3-Br	7-NHC ₂ H ₅	7.92
38	3-Br	7-NMe ₂	7.96
39	3-Br	6,7-di-NH ₂	9.92
40	3-Br	6-NH ₂ ,7-NHMe	9.16
41	3-Br	6-NH ₂ ,7-NMe ₂	6.8
42	3-Br	6-NH ₂ ,7-OMe	8.42
43	3-Br	6-NH ₂ ,7-Cl	8.19
44	3-Br	6-NO ₂ ,7-NH ₂	7.28
45	3-Br	6-NO ₂ ,7-NHMe	7.17
46	3-Br	6-NO ₂ ,7-NMe ₂	5.7
47	3-Br	6-NO ₂ ,7-OMe	7.82
48	3-Br	6-NO ₂ ,7-Cl	7.6
49	3-Br	6,7-di-OHa	9.77
50	3-Br	6,7-di-OC ₂ H ₅	11.22
51	3-Br	6,7-di-OC ₃ H ₇	9.77
52	3-Br	6,7-di-OC ₄ H ₉	6.98
53	3-Br	5,6-di-OMe	5.86

54	3-Br	5,6,7-tri-OMe	9.17
55	2-Br	6,7-di-OMe	6.89
56	4-Br	6,7-di-OMe	9.02
57	3,4-di-Br	6,7-di-OMe	10.14
58	3,5-di-Br	6,7-di-OMe	6.95

Table 2. Calculated values of 2D autocorrelation, RDF, 3D MoRSE, WHIM, and GETAWAY descriptors for the compounds used in present study.

S.No.	MATS1e	MATS3p	RDF110u	RDF095s	Mor29u	G3m	H1i
1	-0.046	-0.122	0.000	0.097	0.176	0.295	2.613
2	-0.051	-0.117	0.000	0.050	0.266	0.193	2.652
3	-0.067	-0.152	0.000	12.376	0.164	0.233	2.585
4	-0.073	-0.141	0.001	6.497	0.263	0.233	2.562
5	-0.061	-0.099	0.587	5.760	0.199	0.255	2.533
6	-0.044	-0.214	0.661	37.934	0.191	0.220	2.188
7	-0.045	-0.119	0.000	0.227	0.150	0.200	2.359
8	-0.066	-0.142	0.001	6.151	0.229	0.200	2.536
9	-0.171	-0.184	0.000	0.334	0.082	0.307	2.765
10	-0.086	-0.256	0.849	35.521	0.000	0.283	2.276
11	-0.186	-0.189	0.002	6.914	0.101	0.188	2.714
12	0.207	-0.178	0.000	0.826	0.076	0.224	2.750
13	0.182	-0.186	0.000	5.764	0.084	0.206	2.695
14	-0.045	-0.119	0.005	2.100	0.245	0.200	2.579
15	-0.066	-0.142	0.000	9.067	0.371	0.184	2.580
16	-0.171	-0.184	0.000	1.043	0.152	0.245	2.749
17	-0.116	-0.179	0.109	1.779	0.094	0.197	2.785
18	-0.164	-0.211	0.018	12.174	0.030	0.206	2.717
19	-0.186	-0.189	0.000	7.948	0.088	0.169	2.695
20	-0.190	-0.121	0.429	7.269	0.069	0.188	2.666
21	-0.086	-0.256	1.790	25.427	0.148	0.197	2.820
22	0.207	-0.178	0.939	3.947	0.234	0.206	2.746
23	0.111	-0.172	0.739	0.936	0.253	0.197	2.790
24	0.159	-0.208	0.000	3.608	0.246	0.188	2.728
25	0.182	-0.186	0.000	9.482	0.336	0.197	2.704
26	0.206	-0.120	0.004	4.865	0.319	0.188	2.683
27	-0.052	-0.105	0.000	2.613	0.326	0.246	2.546
28	-0.065	-0.102	0.025	1.753	0.447	0.191	2.614
29	-0.071	-0.136	0.003	11.858	0.460	0.177	2.666
30	-0.070	-0.132	0.470	15.889	0.330	0.177	2.668
31	-0.059	-0.101	0.041	6.550	0.543	0.162	2.622
32	-0.066	-0.171	2.643	73.531	0.522	0.173	2.665
33	-0.109	-0.109	0.000	8.839	0.226	0.214	2.559
34	-0.040	-0.195	0.005	16.806	0.038	0.198	2.382
35	-0.160	-0.163	0.000	8.544	0.158	0.209	2.628
36	-0.109	-0.109	0.000	16.058	0.369	0.222	2.600
37	-0.088	-0.004	2.740	16.360	0.082	0.184	2.519
38	-0.040	-0.195	0.008	16.883	0.564	0.177	2.535
39	-0.276	-0.219	0.000	10.549	0.227	0.184	2.786
40	-0.199	-0.140	0.003	11.186	0.218	0.193	2.650
41	-0.132	-0.216	0.001	16.226	0.384	0.214	2.576
42	-0.143	-0.177	0.001	11.535	0.216	0.164	2.651
43	-0.178	-0.205	0.000	7.094	0.129	0.206	2.692
44	0.094	-0.219	0.012	11.881	0.272	0.184	2.770

45	0.131	-0.137	0.001	11.248	0.050	0.179	2.634
46	0.163	-0.215	0.001	15.532	0.250	0.187	2.557
47	0.113	-0.175	0.064	12.855	0.166	0.180	2.645
48	0.141	-0.204	0.000	8.518	0.049	0.169	2.672
49	-0.216	-0.182	0.000	8.698	0.173	0.197	2.676
50	-0.043	0.128	1.364	18.212	0.090	0.169	2.543
51	-0.024	0.068	4.719	29.548	-0.171	0.177	2.548
52	-0.010	0.071	8.684	32.772	-0.415	0.182	2.524
53	-0.070	-0.126	1.904	13.297	0.605	0.205	2.709
54	-0.075	-0.112	0.346	12.074	0.378	0.165	2.775
55	-0.070	-0.090	1.679	4.607	0.273	0.191	2.405
56	-0.070	-0.132	0.285	13.644	0.392	0.184	2.733
57	-0.086	0.020	0.828	23.506	0.452	0.177	2.639
58	-0.086	-0.174	1.367	16.717	0.499	0.198	2.723

Table 3. Correlation matrix

	pIC50	MATS1e	MATS3p	RDF110u	RDF095s	Mor29u	G3m	H1i
pIC50	1.000							
MATS1e	-0.602	1.000						
MATS3p	0.331	-0.030	1.000					
RDF110u	0.035	0.022	0.571	1.000				
RDF095s	0.244	-0.079	0.095	0.521	1.000			
Mor29u	0.041	-0.019	-0.176	-0.422	-0.002	1.000		
G3m	-0.462	-0.122	-0.218	-0.163	-0.183	-0.163	1.000	
H1i	0.124	0.048	-0.208	-0.160	-0.291	0.164	-0.181	1.000

Table 4. Regression parameters and quality of correlations

Model No.	Parameters Used	$A_i(1.....6)$	B	Se	R^2	R^2_A	F	Q=R/Se
1	MATS1e	-7.4635(±1.3218)	7.4706	0.1518	0.3628	0.3514	31.883	3.968
2	G3m MATS1e	-26.3556(±3.8767) -8.2836(±0.9905)	12.7199	0.1129	0.6538	0.6412	51.925	7.162
3	G3m MATS1e MATS3p	-24.1464(±3.7812) -8.1400(±0.9433) 3.9631(±1.5146)	12.8520	0.1074	0.6927	0.6756	40.579	7.749
4	G3m MATS1e MATS3p RDF110u	-24.5216(±3.6152) -8.0460(±0.9019) 6.3734(±1.7418) -0.2308(±0.0929)	13.4100	0.1025	0.7248	0.7040	34.895	8.306
5	G3m MATS1e MATS3p RDF095s RDF110u	-22.2852(±3.3394) -7.6033(±0.8275) 8.2819(±1.6698) 0.0356(±0.0101) -0.4418(±0.1033)	12.9503	0.0930	0.7779	0.7566	36.429	9.484
6	G3m H1i MATS1e MATS3p RDF095s RDF110u	-18.9191(±3.2170) 2.6503(±0.7941) -7.4943(±0.7577) 9.8815(±1.6009) 0.0477(±0.0099) -0.4949(±0.0958)	5.4334	0.0851	0.8177	0.7963	38.134	10.626
7	G3m H1i MATS1e MATS3p Mor29u RDF095s RDF110u	-20.5758(±2.8191) 3.2238(±0.7024) -7.4577(±0.6576) 11.0537(±1.4168) -2.1918(±0.5205) 0.0607(±0.0091) -0.7058(±0.0971)	4.8803	0.0738	0.8654	0.8466	45.943	12.605

Table 5. Observed and Estimated pIC₅₀ values using model no 7.(Table 4).

Comp. No.	Obs. pIC ₅₀	Est. pIC ₅₀	Residual
1	6.46	5.85	0.61
2	7.25	7.97	-0.72
3	7.64	7.63	0.01
4	7.57	7.15	0.42
5	7.10	6.66	0.44
6	6.24	6.79	-0.55
7	7.26	7.08	0.19
8	7.52	7.73	-0.21
9	6.11	6.56	-0.45
10	6.24	5.76	0.48
11	9.11	9.26	-0.15
12	5.30	5.51	-0.21
13	6.05	6.08	-0.03
14	6.92	7.69	-0.77
15	8.00	8.07	-0.07
16	7.00	7.67	-0.67
17	8.70	8.52	0.18
18	9.60	8.95	0.65
19	10.00	9.68	0.32
20	9.46	9.67	-0.21
21	8.48	7.69	0.80
22	4.92	5.05	-0.13
23	5.22	6.07	-0.85
24	6.09	6.00	0.09
25	6.00	5.97	0.03
26	6.27	6.39	-0.12
27	7.54	6.70	0.84
28	8.42	7.84	0.58
29	9.51	8.57	0.94
30	10.60	8.81	1.79
31	9.05	8.50	0.55
32	9.62	9.97	-0.35
33	8.40	8.38	0.02
34	7.08	7.56	-0.48
35	8.33	8.62	-0.29
36	8.16	8.47	-0.31
37	7.92	8.71	-0.79
38	7.96	7.34	0.62
39	9.92	9.86	0.06
40	9.16	9.59	-0.43
41	6.80	7.52	-0.72
42	8.42	9.39	-0.97
43	8.19	8.53	-0.34
44	7.28	7.02	0.26
45	7.17	7.77	-0.60
46	5.70	6.08	-0.38
47	7.82	7.30	0.52
48	7.60	7.12	0.48
49	9.77	9.20	0.57
50	11.22	11.28	-0.06
51	9.77	9.22	0.55
52	6.98	6.90	0.08
53	5.86	6.66	-0.80
54	9.17	9.41	-0.24
55	6.89	6.73	0.16
56	9.02	8.74	0.28
57	10.14	10.46	-0.32
58	6.95	7.26	-0.31

Table 6. Cross validated parameters for the best obtained models.

Model No.	Parameters used	PRESS/SSY	R ² _{cv}	S _{PRESS}	PSE
1	MATS1e	1.7564	-0.7564	1.1855	1.1649
2	G3m MATS1e	0.5296	0.4704	0.8818	0.8587
3	G3m MATS1e	0.4436	0.5564	0.7028	0.8089

	MATS3p				
4	G3m MATS1e MATS3p RDF110u	0.3797	0.6203	0.8008	0.7655
5	G3m MATS1e MATS3p RDF095s RDF110u	0.2855	0.7145	0.7263	0.6877
6	G3m H1i MATS1e MATS3p RDF095s RDF110u	0.2229	0.7771	0.6644	0.6230
7	G3m H1i MATS1e MATS3p Mor29u RDF095s RDF110u	0.1555	0.8445	0.5765	0.5353

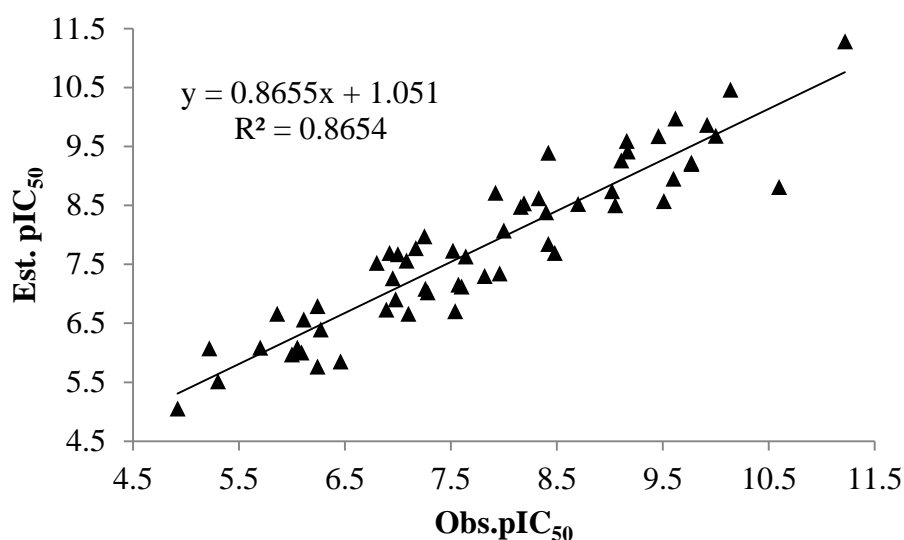


Figure 2. Correlation between Observed and estimated pIC_{50} activity using model 7 (Table 4).

Table 7. Ridge analysis for the best seven-parametric model.

Model No.	Parameters used	VIF	Tolerance	Eigenvalue	Condition no.
7	MATS1e	1.0464	0.9556	2.1416	1.00
	MATS3p	1.9491	0.5131	1.3253	1.62
	RDF110u	3.1378	0.3187	1.1028	1.94
	RDF095s	2.0512	0.4875	0.9363	2.29
	Mor29u	1.4864	0.6728	0.7875	2.72
	G3m	1.2557	0.7964	0.5377	3.98
	H1i	1.3308	0.7515	0.1685	12.70

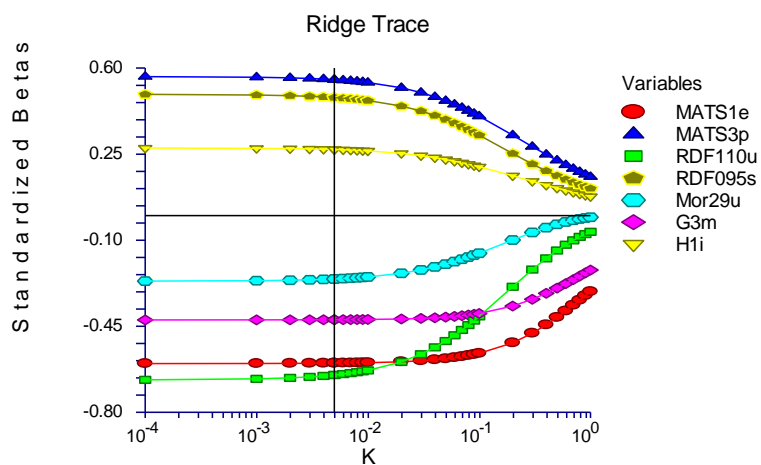


Fig 3: Ridge trace for seven variable model 7 (Table 4)

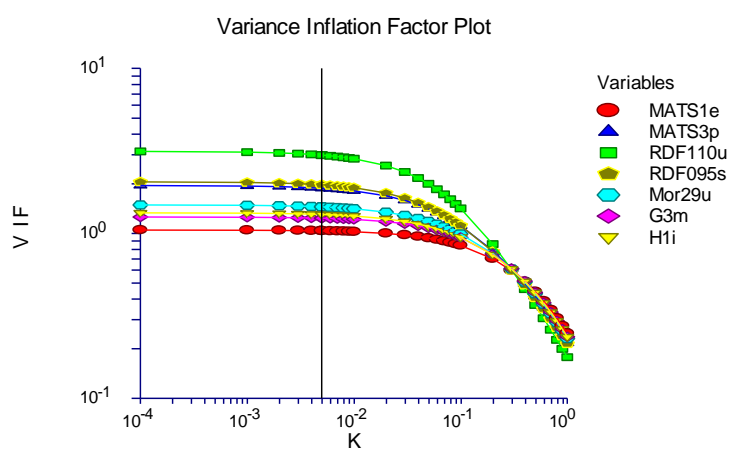


Fig 4: VIF plot for seven variable model-7(Table 4)